

## **Supplemental Appendix**

**Supplemental Material and Methods, pages 2-9**

**Supplemental Table 1, page 10**

**Supplemental Table 2, pages 11-12**

**Supplemental Figures 1-5, pages 13-17**

**Supplemental References, page 18**

# 1 **Materials and methods**

## 2 *Study population*

3 Seventeen hospitalized patients due to COVID-19 were prospectively recruited from Karolinska  
4 University Hospital, Stockholm. To minimize the confounding effects of comorbidities, we  
5 attempted to include patients with moderate infection but still requiring hospital care (i.e. only  
6 reason for hospitalization is oxygen demand and no other organ failure than respiratory). Inclusion  
7 criteria were: age >18 years, PCR-verified SARS-CoV-2 infection within the last 14 days,  
8 pulmonary COVID-19 associated interstitial infiltrates on x-ray, requiring in-hospital care, oxygen  
9 demand during hospital stay, and hospital arrival within the last 14 days. Exclusion criteria were:  
10 type 1 or 2 diabetes, myocardial infarction within the last 6 months, acute kidney injury, chronic  
11 kidney disease, pregnancy, ongoing malignancy, >1 cardiopulmonary comorbidity, unwillingness  
12 to participate, need for intensive care, mechanical ventilation or non-invasive ventilation. Clinical  
13 and demographic characteristics were collected from subjects' medical charts. For routine clinical  
14 blood analyses that were analyzed several times during the hospital stay, samples taken on the day  
15 of inclusion or one day before/after inclusion were recorded and presented in Table 1. Fourteen of  
16 the COVID-19 patients underwent additional venous blood sampling after an overnight fasting.  
17 Following recovery from the infection, ten subjects were scheduled for a follow-up visit after 4  
18 months. Routine clinical chemistry and hemodynamic parameters were recorded during this visit.  
19 Twenty-seven healthy Age- and sex-matched controls were included. All subjects were informed  
20 of the nature, purpose, and possible risks involved in the study. Oral and written informed consent  
21 were obtained from all study participants prior to inclusion. The study was conducted according  
22 to the declaration of Helsinki and approved by the Swedish Ethical Review Authority.

23

24 *Peripheral endothelial function testing*

25 Fifteen of the COVID-19 patients and 14 of the healthy controls were included for determination  
26 of peripheral endothelial function. Following recovery from the infection, ten COVID-19 patients  
27 underwent additional evaluation of reactive hyperemia index (RHI) four months later. The subjects  
28 were asked to refrain from caffeine-containing drinks or tobacco consumption 12h prior to the  
29 investigation. Non-invasive determination of endothelial function was performed with pulse  
30 amplitude tonometry (PAT) device placed on the tip of each finger (Endo-PAT2000; Itamar  
31 Medical, Caesarea, Israel). Following 10 min of rest in the supine position, the PAT signal was  
32 recorded at baseline and following 5 min circulatory occlusion of one forearm by a blood pressure  
33 cuff inflated to 60 mmHg suprasystolic pressure or at least 200 mmHg. The contralateral arm  
34 served as control. The post-occlusive hyperemia causes endothelium-dependent vasodilatation  
35 through nitric oxide (NO) release [1]. PAT signal was recorded simultaneously in both fingers and  
36 the change in pulse amplitude from baseline measurement in the active arm divided by the  
37 contralateral arm is expressed as RHI, which reflects digital microvascular endothelial function  
38 and predicts cardiovascular events [2].

39

40 *Animals and vessel isolation*

41 Male Wistar rats (Charles River, Sulzfeld, Germany) age of 9-18 weeks at sacrifice were housed  
42 in the animal facility (Comparative Medicine Biomedicum) of Karolinska Institutet and kept in a  
43 12:12-hour light-dark cycles with free access to standard chow and water. Animal care and all  
44 protocols were approved by the Regional Ethical Committee and conformed to the Guide for Care  
45 and Use of Laboratory Animals published by the US National Institutes of Health (NIH publication  
46 NO. 85-23, revised 1996). Rats were anesthetized with pentobarbital sodium (50 mg/kg i.p.)

47 followed by thoracotomy and removal of aortas. The aortas were then cleaned from adipose and  
48 connective tissues, cut transversely into 2 mm rings, and were used in the experiments described  
49 below.

50

#### 51 *RBC isolation and incubation*

52 Whole blood was collected from study participants in heparinized tubes through the cubital vein.  
53 RBCs were isolated and incubated with isolated aortic rings as previously described [3]. Briefly,  
54 whole blood from COVID-19 patients (in the acute phase and at follow-up) and healthy subjects  
55 underwent centrifugation at 1000g at 4°C for 10 min followed by removal of plasma and buffy  
56 coat. Subsequently, three cycles of washing (with centrifugation at 1000g at 4°C for 5 min per each  
57 cycle) with Krebs-Henseleit (KH) buffer (pH 7.4) containing (in mM): 118 NaCl, 4.7 KCl, 1.2  
58 MgSO<sub>4</sub>, 1.2 KH<sub>2</sub>PO<sub>2</sub>, 25 NaHCO<sub>3</sub>, 11 glucose, and 2.4 CaCl<sub>2</sub> were conducted to obtain isolated  
59 RBCs. Previous analyses revealed that this protocol removes >98% of platelets and >99% of  
60 leukocytes [4]. Isolated RBCs were stored at -80°C until further analyses or diluted to a hematocrit  
61 of ~45% with KH-buffer and incubated with isolated aortic segments for 18h at 37°C, 95% O<sub>2</sub>,  
62 and 5% CO<sub>2</sub> in the absence or presence of TEMPOL, *see below*. Following the thorough removal  
63 of RBCs, vessel rings were mounted in myograph organ chambers immediately for vessel  
64 reactivity experiments or fixed with 4% formaldehyde for immunohistochemistry.

65

#### 66 *Plasma isolation and incubation*

67 Plasma was isolated from whole blood in EDTA tubes following centrifugation at 1000g at 4°C  
68 for 10 min and stored at -80°C. On the day of the experiments, plasma was diluted to a  
69 concentration of 5% with KH-buffer and co-incubated with isolated aortic rings for 18h at 37°C,

70 95% O<sub>2</sub>, and 5% CO<sub>2</sub> according to previously [5, 6]. After washing, the aortic rings were mounted  
71 in myograph organ chambers for vessel reactivity experiments as described below. In separate sets,  
72 vessel reactivity experiments were performed with 5% plasma present in the organ chamber for 1h  
73 with subsequent washing x3 prior to evaluation of endothelium-dependent relaxation.

74

#### 75 *Vessel reactivity experiments*

76 Aortic rings incubated with RBCs either from healthy subjects (H-RBCs) or from COVID-19  
77 patients (C19-RBCs) were mounted in isolated organ chambers (Danish Myo Technology A/S,  
78 Hinnerup, Denmark) following thorough washing. Contractile forces were recorded with Harvard  
79 isometric transducer (Harvard Apparatus, Holliston, MA). Internal diameter was set to 0.9 times  
80 the estimated diameter of 100 mmHg followed by an equilibrium period of ~30min. Vessels were  
81 then exposed to KCl twice (50 mM and 100 mM). Endothelium-dependent relaxation (EDR) was  
82 evaluated by cumulative increase in concentrations of acetylcholine (ACh, 1 nM-10 μM) following  
83 precontraction of the vessel by the combined administration of the thromboxane analogue 9,11-  
84 Dideoxy-9α,11α-methanoepoxyprostaglandin F<sub>2α</sub> (U46619) and/or phenylephrine. Endothelium-  
85 independent relaxation (EIR) was evoked by the administration of increasing concentrations (1  
86 nM-10 μM) of sodium nitroprusside (SNP), or at the end of the experiment following evaluation  
87 of EDR with one dose (10 μM). Previous experiments have shown that human RBCs can be  
88 incubated with rat arteries without affecting vascular function *per se*, and that similar responses  
89 are obtained in rat and human arteries [3]. EDR and EIR evaluations were performed in the absence  
90 and presence of the arginase inhibitor 2(S)-amino-6-borono-hexanoic acid (ABH, 100 μM), the  
91 superoxide dismutase mimetic 4-hydroxy-2,2,6,6-tetramethylpiperidine-N-oxyl (TEMPOL, 100  
92 μM), and the inhibitor of NADPH oxidases (NOXs) apocynin (100 μM). The compounds were

93 present for 1h in the organ chamber after the 18h incubation prior to evaluation of EDR and EIR  
94 to elucidate the contribution of vascular arginase/superoxide/NOX. TEMPOL (10 mM) was also  
95 applied during the 18h co-incubation of RBCs and aortic segments to selectively investigate the  
96 contribution of RBC superoxide. We have previously shown that these pharmacological  
97 compounds do not affect EDR or EIR incubated with RBCs from healthy subjects and that this  
98 protocol does not result in any carry-over effect of attenuation of ROS to the aorta [3].

99 In a separate set of experiments, washed H-RBCs were pre-incubated for 2h at 37°C in the  
100 absence and presence of recombinant interferon (IFN) $\gamma$ , tumor necrosis factor (TNF) $\alpha$ , interleukin  
101 (IL)-9, or macrophage inflammatory protein (MIP)-1 $\beta$  at concentrations of 100 ng/ml or 500 ng/ml  
102 at a hematocrit of ~45%. Following centrifugation at 300g at 37°C for 5 min and one washing  
103 cycle with KH buffer, RBCs were diluted to a hematocrit of 45% with KH buffer and incubated  
104 with aortic segments for 18h. EDR and EIR were then evaluated as explained above.

105

#### 106 *Immunohistochemistry*

107 Following the RBC incubation for 18h, rat aortic rings were fixed for 24h in 4% formaldehyde at  
108 room temperature, dehydrated in graded ethanol (70, 95, and 99%), embedded in paraffin,  
109 sectioned using a microtome, and mounted on coated glass slides (Superfrost® plus; Thermo  
110 Fisher Scientific, Waltham, MA). At least 6 slides, containing ~4 tissue cross-sections (5- $\mu$ m thick)  
111 from each animal were examined. Sections were deparaffinized in xylene and rehydrated in graded  
112 ethanol. For antigen retrieval, slides were subjected to high-pressure boiling in citrate buffer (pH  
113 6.0). After peroxidase inactivation (0.3%) and blockade with goat serum (Abcam, Cambridge,  
114 UK), aorta cross-sections were incubated overnight (4°C) with the following primary antibodies:  
115 a rabbit polyclonal anti-human arginase 1 (1:100 dilution, catalog No. HPA003595, Atlas Prestige

116 Antibody, Sigma-Aldrich, St. Louis, MO) and a mouse monoclonal anti-4-Hydroxynonenal  
117 (HNE) antibody (1:100 dilution, IgG<sub>2B</sub>, catalog No. MAB3249; R&D Systems, Inc., Minneapolis,  
118 MN). Specific labeling was detected using a labeled horseradish peroxidase (HRP) polymer-  
119 conjugate as a secondary antibody as part of the EnVision<sup>+</sup> Dual Link System-HRP (Dako, Agilent  
120 Technologies, Santa Clara, CA). To confirm the specificity of antibodies, isotype controls were  
121 used as negative controls (rabbit IgG or mouse IgG<sub>2B</sub>, both from Abcam). Samples were  
122 developed using a solution containing 3, 3'-diaminobenzidine (DAB, Dako), then counterstained  
123 with Mayer's Modified Hematoxylin (Abcam), and mounted in mounting medium  
124 (Abcam). Fields from each aortic section were captured (Leica DM3000 Digital microscope; Leica  
125 Biosystems, Wetzlar, Germany), digitized, and analyzed (*ImageJ* software 1.52v, Bethesda, MA).  
126 Positive areas were quantified for either both intima and media layers (total) or only endothelial  
127 cells as previously described [7]. Adventitial layers were not included for quantification.

128

### 129 *Detection of reactive oxygen species with electron spin resonance*

130 ROS formation in RBCs was determined using electron spin resonance (ESR) as previously  
131 described [3]. Briefly, washed RBCs were diluted to a hematocrit of 1% with Krebs/HEPES-  
132 buffer. The RBCs were incubated with 1-hydroxy-3-methoxycarbonyl-2,2,5,5-  
133 tetramethylpyrrolidine (CMH, 200  $\mu$ M) in the presence of 25  $\mu$ M desferoxamine and 5  $\mu$ M  
134 diethyldithiocarbamate (Noxygen Science Transfer & Diagnostics GmbH, Elzach, Germany) for  
135 30 min at 37°C and 21% O<sub>2</sub>. The cell suspensions were then frozen in liquid nitrogen and stored  
136 at -80°C until analyses. ROS formation was detected by ESR using the following setting: center  
137 field 1.99 g, microwave power 1 mW, modulation amplitude 9 G, sweep time 10 s, number of

138 scans 10, field sweep 60 G. The amount of CM• was determined from the calibration using 3-  
139 carboxy-proxyl (CP•, Noxygen Science Transfer & Diagnostics GmbH).

140

#### 141 *Nitrate determination*

142 H-RBCs and C19-RBCs were diluted with KH-buffer to a hematocrit of 5% and incubated for 30  
143 min at 37°C in the presence and absence of ABH at 0.1 mM or 1 mM in nitrate-free Eppendorf  
144 tubes. Following incubation, the samples were centrifuged at 1000g for 10 min at 4°C, and  
145 supernatants were stored at -80°C until analyzed. Nitrate was measured with a dedicated high-  
146 performance liquid chromatography system (ENO-20; EiCom, Kyoto, Japan) as previously  
147 described [8]. Prior to measurements, all samples were heated at 56°C for 45 min to inactivate the  
148 possible remaining virus. Control experiments revealed that nitrate levels are not affected by this  
149 heating procedure.

150

#### 151 *Cytokine profiling*

152 Stored H-RBCs and C19-RBCs underwent three freeze-thaw cycles before analysis to ensure  
153 complete lysis according to previously [9]. Lysates were diluted in PBS supplemented with 0.5%  
154 bovine serum albumin on the day of experiment. 27-plex assay (#M500KCAF0Y; Bio-Rad,  
155 Hercules, CA) for IL-1 $\beta$ , interleukin-1 receptor antagonist (IL-1ra), IL-2, IL-4, IL-5, IL-6, IL-7,  
156 IL-8, IL-9, IL-10, IL-12, IL-13, IL-15, IL-17, Eotaxin, fibroblast growth factor (FGF) basic,  
157 granulocyte colony-stimulating factor (G-CSF), granulocyte-macrophage colony-stimulating  
158 factor (GM-CSF), IFN $\gamma$ , interferon  $\gamma$  induced protein-10 (IP-10), monocyte chemoattractant  
159 protein-1 (MCP-1), MIP-1 $\alpha$ , platelet-derived growth factor (PDGF), MIP-1 $\beta$ , regulated on  
160 activation, normal T cell expressed and secreted (RANTES), TNF $\alpha$ , and vascular endothelial



161 growth factor (VEGF) was performed according to manufacturer's instructions using Bio-Plex®  
162 handheld magnetic washer (Bio-Rad). The assay was run on the Luminex® 200™ (Luminex  
163 Corporate, Austin, TX).

164

165 *Free hemoglobin in plasma*

166 The concentrations of free hemoglobin in plasma from healthy subjects and COVID-19 patients  
167 both at the acute phase and follow-up were quantified via a commercial immunoassay kit (ELISA;  
168 Bethyl Laboratories, Montgomery, TX) according to the manufacturer's instructions.

Supplemental Table 1. Change in hemodynamic and laboratory parameters at follow-up.

	Acute phase n=10	Follow-up n=10	p-value
Age (years)	54 ± 12	54 ± 12	0.343 (a)
Male, n (%)	8 (80)	8 (80)	
BMI (kg/m <sup>2</sup> )	30 ± 4	31 ± 4	0.041 (a)
Co-existing conditions:			
Hypertension, n (%)	3 (30)	3 (30)	
Previous myocardial infarction, n (%)	1 (10)	1 (10)	
Asthma or COPD, n (%)	0 (0)	0 (0)	
Hemodynamic parameters			
SBP (mmHg)	118 ± 12	131 ± 14	0.027 (a)
DBP (mmHg)	76 (65-86)	86 (80-94)	0.004 (b)
Heart rate (beats/min)	73 ± 17	70 ± 12	0.599 (a)
Respiratory rate (breaths/min)	19 ± 3	17 ± 2	0.255 (a)
Oxygen saturation (%)	94 ± 3	97 ± 1	0.029 (a)
Erythrocyte indices			
Hemoglobin (g/L)	135 (125-142)	145 (130-153)	0.006 (b)
EVF	0.39 ± 0.03	0.43 ± 0.03	<0.001 (a)
MCV (fL)	87 (82-89)	87 (83-89)	0.531 (b)
MCH (pg)	30 (28-30)	29 (28-30)	0.750 (b)
RBC count (10 <sup>12</sup> /L)	4.7 ± 0.4	4.9 ± 0.5	0.115 (a)
Thrombocytes (10 <sup>9</sup> /L)	364 (290-474)	216 (171-281)	0.019 (b)

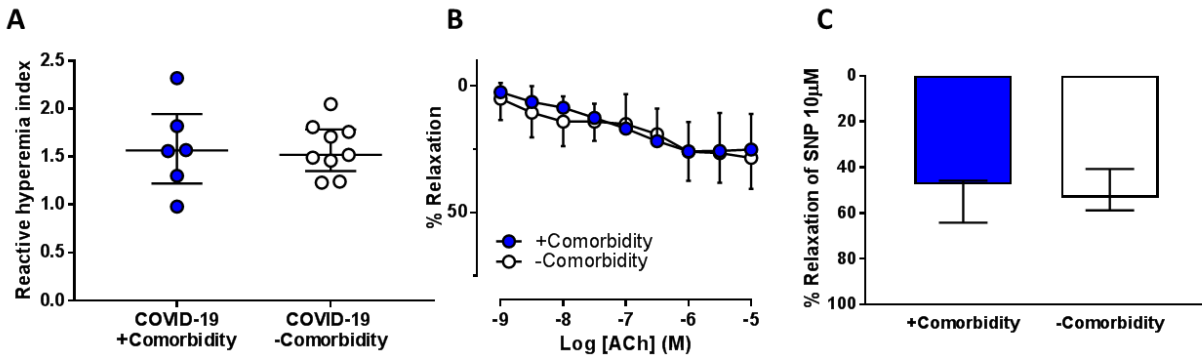
Values are median (Q1-Q3), mean ± SD, or count, n (%) unless otherwise stated. BMI - body mass index, COPD - chronic obstructive pulmonary disease, DBP - diastolic blood pressure, EVF - erythrocyte volume fraction, MCH - mean corpuscular hemoglobin, MCV - mean corpuscular volume, mmHg - millimeter mercury, RBC - red blood cell, SBP - systolic blood pressure. *a* indicates paired t-test and *b* indicates Wilcoxon signed-rank test.

Supplemental Table 2. Panel of cytokines in lysed RBCs from healthy (H-RBCs) or COVID-19 patients (C19-RBCs).

Cytokine	H-RBCs (pg/ml RBC lysate)	H-RBCs >LLOQ of n=10	H- RBCs >LOD of n=10	C19-RBCs (pg/ml RBC lysate)	C19- RBCs >LLOQ of n=10	C19- RBCs >LOD of n=10
IL-1 $\beta$	2.2	1	6	4.4 (4.0-5.2)	6	10
IL-1ra	3629 (3167- 4217)	10	10	2370 (1665-6650)	10	10
IL-2	-	0	0	-	0	0
IL-4	-	0	1	-	1	1
IL-5	73 (70-76)	2	4	79 (65-99)	3	7
IL-6	-	0	1	-	0	0
IL-7	-	0	3	25 (24-25)	2	6
IL-8	7.8	1	10	13.3 (11.4-16.3)	5	10
IL-9	27 (17-47)	8	10	190 (149-273)***	10	10
IL-10	-	0	10	7.7 (7.0-8.3)	2	10
IL-12	-	0	3	-	0	2
IL-13	-	0	1	-	0	1
IL-15	-	0	0	-	0	0
IL-17	-	0	10	-	0	10
Eotaxin	11.0 (8.7-14.3)	10	10	9.6 (4.7-17.3)	10	10
FGF basic	-	0	1	49	1	5
G-CSF	42 (40-43)	4	9	43 (40-45)	7	10
GM-CSF	-	0	1	5.7	1	1
IFN $\gamma$	-	0	0	-	0	9***
IP-10	16.9 (15.6-21.1)	3	10	17.4 (15.5-29.1)	4	10
MCP-1	111 (89-173)	10	10	147 (98-202)	10	10
MIP-1 $\alpha$	-	0	6	-	0	6
PDGF	208 (169-294)	10	10	597 (301-913)	10	10
MIP-1 $\beta$	9.5 (4.8-12.0)	8	9	81.7 (63.5- 102.0)***	10	10
RANTES	268 (136-340)	10	10	1135 (806-2226)	10	10
TNF $\alpha$	-	0	2	-	0	9**
VEGF	490 (228-536)	10	10	358 (307-563)	10	10

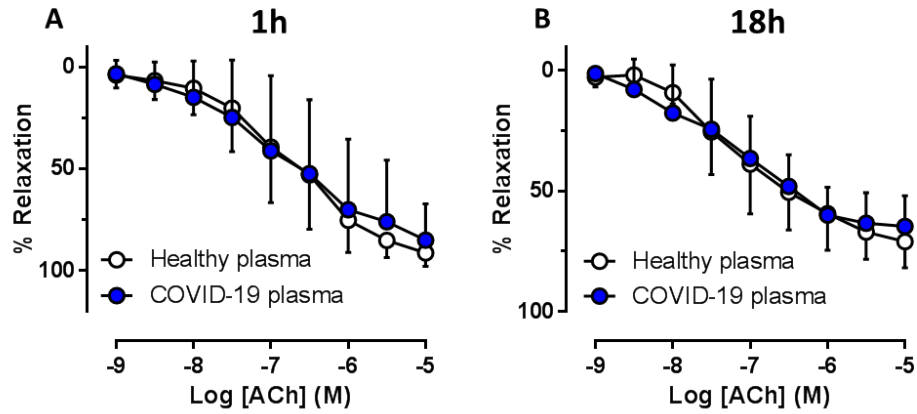
Continuous variables are presented as median (Q1-Q3) or single value if at least one value in the group was above the lower limit of quantitation (LLOQ). Number(s) of samples >LLOQ and >limit of detection (LOD) are also presented for the groups. Statistical comparison for continuous variables between the groups was carried out with Mann-Whitney test if both groups had at least n=3 values and categorical data (number of samples of which cytokine levels were >LOD) was carried out with Fisher's exact test. \*\*p<0.01, \*\*\*p<0.001 vs. H-RBCs. FGF - fibroblast growth factor, G-CSF - granulocyte colony-stimulating factor, GM-CSF - granulocyte-macrophage

colony-stimulating factor, IFN $\gamma$  - interferon  $\gamma$ , IL - interleukin, IL-1ra - interleukin-1 receptor antagonist, IP-10 - interferon  $\gamma$  induced protein-10, MCP-1 - monocyte chemoattractant protein-1, MIP - macrophage inflammatory protein, PDGF - platelet-derived growth factor, RANTES - regulated on activation, normal T cell expressed and secreted, TNF $\alpha$  - tumor necrosis factor  $\alpha$ , VEGF - vascular endothelial growth factor.



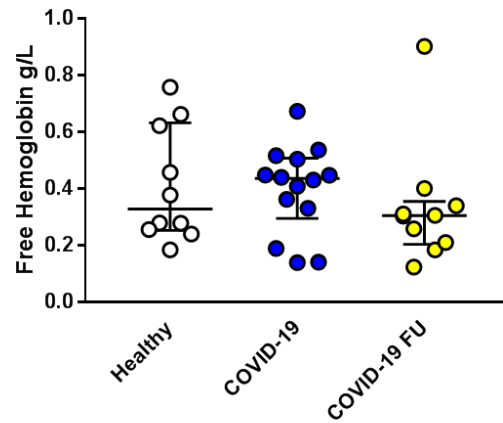
**Supplemental Figure 1. Influence of comorbidities on RHI and C19-RBCs induced vascular dysfunction.**

Subgroup analyses of RHI in the patients within the COVID-19 group without (-, n=9) compared to with (+, n=6) comorbidity (A). Endothelium-dependent relaxations (B), and endothelium-independent relaxations (C) in aortic rings following 18h incubation with RBCs from patients within the COVID-19 (C19-RBCs) group without (-, n=8) and with (+, n=6) comorbidity. The patients in the comorbidity group consisted of: hypertension (n=4), chronic obstructive pulmonary disease (n=1), and previous myocardial infarction (n=1). Mann-Whitney test (A and C) and two-way ANOVA (B) were used for statistical analysis between groups. No significant differences were detected. Values are expressed as median (Q1-Q3) (A and C) or mean and SD (B).



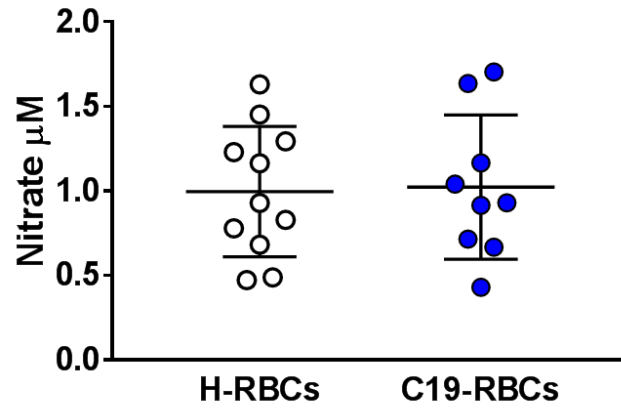
**Supplemental Figure 2.** Plasma from patients with COVID-19 does not affect endothelium-dependent relaxation.

Endothelium-dependent relaxation in aortic rings following 1h (A, n=8 in each group) or 18h incubation (B, n=4 in each group) with plasma from healthy subjects or patients with COVID-19. Two-way ANOVA was used for statistical analysis between groups. No significant differences were detected. Values are expressed as mean and SD.



**Supplemental Figure 3. Free hemoglobin in plasma.**

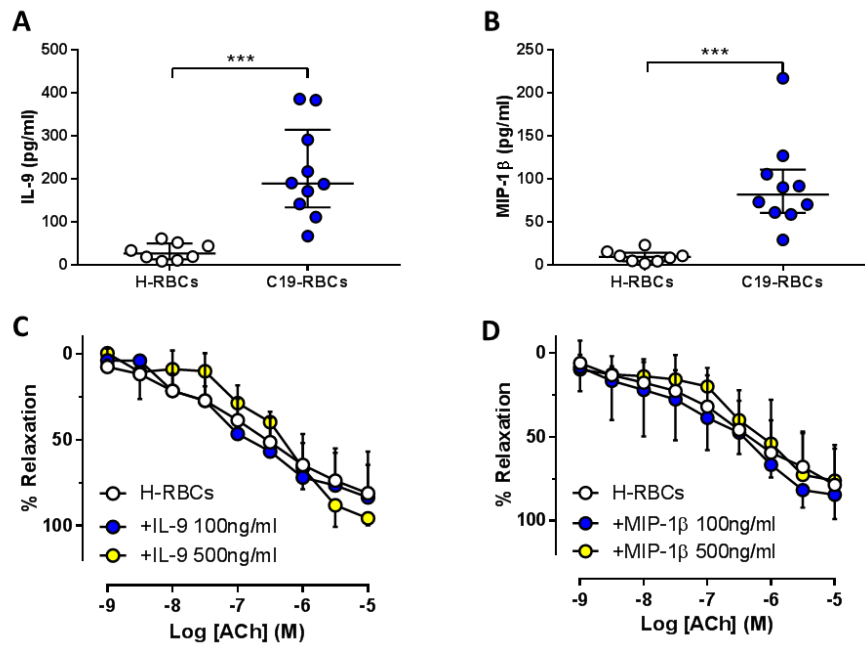
Free hemoglobin in plasma from healthy subjects (n=10), patients with COVID-19 in the acute phase (COVID-19, n=14), and at follow-up (COVID-19 FU, n=10). Kruskal-Wallis test with Dunn's multiple comparison test was used. No significant differences between groups were detected. Values are expressed as median (Q1-Q3).



**Supplemental Figure 4.** Baseline nitrate levels in RBCs.

Baseline nitrate levels in the supernatant following incubation with H-RBCs or C19-RBCs (n=9-11). Unpaired t-test was used. No significant difference between groups. Values are expressed as mean  $\pm$  SD.





**Supplemental Figure 5. Interleukin-9 and macrophage inflammatory protein-1β in RBCs.**

Levels of interleukin (IL)-9 (A) and macrophage inflammatory protein (MIP)-1β (B) in H-RBCs and C19-RBCs. Effect of 2h pre-incubation of H-RBCs with (C) IL-9 (n=3-4), and (D) MIP-1β (n=3-5) on endothelium-dependent relaxations induced by ACh. Values are expressed as median (Q1-Q3) (A and B) and mean and SD (C and D). \*\*\*p<0.001 as indicated with Mann-Whitney test. Two-way ANOVA matched for both concentration and relaxation with Dunnett's post hoc test were used in C and D, with no statistical differences.

## References (Supplemental Appendix)

- 1 Hamburg NM, Benjamin EJ. Assessment of endothelial function using digital pulse amplitude tonometry. *Trends Cardiovasc Med* 2009; **19**: 6-11.
- 2 Alexander Y, Osto E, Schmidt-Trucksass A, *et al.* Endothelial function in cardiovascular medicine: a consensus paper of the European Society of Cardiology Working Groups on Atherosclerosis and Vascular Biology, Aorta and Peripheral Vascular Diseases, Coronary Pathophysiology and Microcirculation, and Thrombosis. *Cardiovasc Res* 2021; **117**: 29-42.
- 3 Zhou Z, Mahdi A, Tratsiakovich Y, *et al.* Erythrocytes From Patients With Type 2 Diabetes Induce Endothelial Dysfunction Via Arginase I. *J Am Coll Cardiol* 2018; **72**: 769-80.
- 4 Yang J, Gonon AT, Sjoquist PO, Lundberg JO, Pernow J. Arginase regulates red blood cell nitric oxide synthase and export of cardioprotective nitric oxide bioactivity. *Proc Natl Acad Sci U S A* 2013; **110**: 15049-54.
- 5 McCann Haworth SM, Zhuge Z, Nihlen C, *et al.* Red blood cells from patients with pre-eclampsia induce endothelial dysfunction. *J Hypertens* 2021; **39**: 1628-41.
- 6 Hayman R, Warren A, Brockelsby J, Johnson I, Baker P. Plasma from women with pre-eclampsia induces an in vitro alteration in the endothelium-dependent behaviour of myometrial resistance arteries. *BJOG* 2000; **107**: 108-15.
- 7 Ding Y, Huang L, Xian X, *et al.* Loss of Reelin protects against atherosclerosis by reducing leukocyte-endothelial cell adhesion and lesion macrophage accumulation. *Sci Signal* 2016; **9**: ra29.
- 8 Montenegro MF, Sundqvist ML, Nihlen C, Hezel M, Carlstrom M, Weitzberg E, Lundberg JO. Profound differences between humans and rodents in the ability to concentrate salivary nitrate: Implications for translational research. *Redox Biol* 2016; **10**: 206-10.
- 9 Karsten E, Breen E, Herbert BR. Red blood cells are dynamic reservoirs of cytokines. *Sci Rep* 2018; **8**: 3101.